The lattice Boltzmann method in acoustics

Erlend Magnus Viggen
Acoustics Group, Department of Electronics and Telecommunications, NTNU, O.S. Bragstads Plass 2, 7034 Trondheim, Norway

(Dated: Presented at SSPA10 9 February 2010)

The lattice Boltzmann method, a method based in kinetic theory and used for simulating fluid behaviour, is presented with particular regard to usage in acoustics. A point source method of generating acoustic waves in the computational domain is presented, and simple simulation results with this method are analysed. The simulated waves' transient wavefronts in one dimension are shown to agree with analytical solutions from acoustic theory. The phase velocity and absorption coefficients of the waves and their deviations from theory are analysed. Finally, the physical time and space steps relating simulation units with physical units are discussed and shown to limit acoustic usage of the method to small scales in time and space.

I. INTRODUCTION

We can subdivide numerical methods in acoustics into two main types:

Top-down methods which attempt to find a solution to a set of differential equations by different methods of discretisation (e.g. finite difference and finite element methods).

Bottom-up methods which compute microscale algorithms which give rise to macroscale physical behaviour (e.g. cellular automata, the TLM method, lattice gas automata, lattice Boltzmann method).

The lattice Boltzmann method is of the latter type, being based in mesoscopic kinetic theory and used for simulations of macroscopic behaviour. It can be seen as either an evolution of the older method of lattice gas automata, or as a discretisation of the Boltzmann equation, which is a fundament of kinetic theory. The method works by tracking the movement and interaction of particle distributions inside the computational domain.

Since its beginning in 1988,[1] the method has been used for a number of acoustically related purposes, including simulations of acoustic streaming,[2,3] shock fronts,[4] particle motion in ultrasound fields,[5] flow simulations in reed instrument mouthpieces,[6] and investigation of glottal flow.[7]

II. LATTICE BOLTZMANN BACKGROUND

A d-dimensional domain is discretised by an evenly spaced lattice, defined by q different lattice vectors $\mathbf{c}_i$, which also represent possible particle velocities. Each node contains q different particle distributions $f_i(\mathbf{x}, t)$, each representing the density of particles at position $\mathbf{x}$ and time t with velocity $\mathbf{c}_i$.

From these particle distributions, we can find each node's macroscopic quantities of density and momentum. The density ρ is found by summing the particle distributions at a node,

$$\rho(\mathbf{x}, t) = \sum_i f_i(\mathbf{x}, t), \tag{1}$$

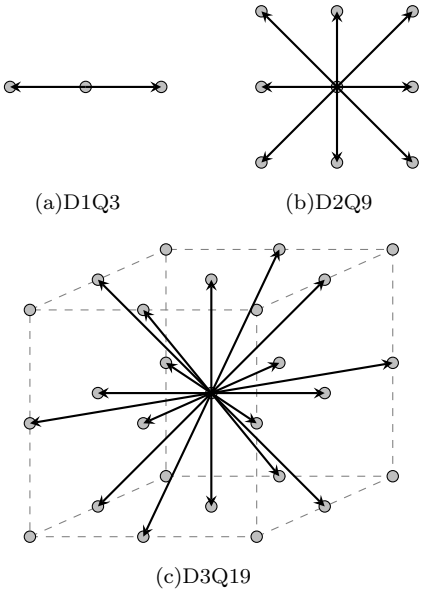

(a)D1Q3 (b)D2Q9

(c)D3Q19

FIG. 1. Velocity vectors in different lattices. Rest vectors $\mathbf{c}_0 = \mathbf{0}$ are not indicated.

while momentum is found by summing the individual momenta of each particle distribution,

$$\rho(\mathbf{x}, t)\mathbf{u}(\mathbf{x}, t) = \sum_i \mathbf{c}_i f_i(\mathbf{x}, t), \tag{2}$$

where $\mathbf{u}$ is particle velocity.

A lattice is characterised by its number of dimensions d and its number of velocity vectors q, and is denoted by DdQq. Fig. 1 and Table I show the different velocity vectors in the common D1Q3, D2Q9, and D3Q19 lattices.

The method's time step update is described by the lattice Boltzmann evolution equation,

$$f_i(\mathbf{x} + \mathbf{c}_i, t + 1) = f_i(\mathbf{x}, t) + \Omega_i(\mathbf{x}, t). \tag{3}$$

This equation states that incoming particle distributions $f_i(\mathbf{x}, t)$ are streamed to neighbouring nodes in their direction of velocity, after being modified by the collision

TABLE I. Basic velocity vectors and their weighting factors for the three lattices used in this article. The complete set of vectors is all possible spatial permutations of the basic vectors given here.

(a) D1Q3

$\mathbf{c}_i$	t_i
(0)	2/3
(±1)	1/6

(b) D2Q9

$\mathbf{c}_i$	t_i
(0, 0)	4/9
(±1, 0)	1/9
(±1, ±1)	1/36

(c) D3Q19

$\mathbf{c}_i$	t_i
(0, 0, 0)	1/3
(±1, 0, 0)	1/18
(±1, ±1, 0)	1/36

operator $\Omega_i(\mathbf{x}, t)$. This collision operator represents collisions by redistributing particles between distributions in such a way that conservation of mass and momentum is upheld.

The simplest and most common collision operator is the lattice Bhatnagar-Gross-Krook (LBGK) operator,

$$\Omega_i = -\frac{1}{\tau}\left[f_i - f_i^{\mathrm{eq}}\right], \tag{4}$$

which is based on relaxation to an equilibrium distribution $f_i^{\mathrm{eq}}(\mathbf{x}, t)$ with a relaxation time τ. We have here simplified our notation by considering $(\mathbf{x}, t)$ implicit. The equilibrium distribution is given by

$$f_i^{\mathrm{eq}} = \rho t_i \left(1 + \frac{\mathbf{u}\cdot\mathbf{c}_i}{c_s^2} + \frac{(\mathbf{u}\cdot\mathbf{c}_i)^2}{2c_s^4} - \frac{\mathbf{u}^2}{2c_s^2}\right), \tag{5}$$

which is the particle distribution which maximises entropy, in analogy with the Maxwell-Boltzmann distribution in gases. The equilibrium distribution is constructed from the node's pre-collision values of ρ and $\mathbf{u}$. c_s is the lattice speed of sound, which is equal to $1/\sqrt{3}$ for the lattices given in Table I and Figure 1, while t_i is a weighting factor which ensures that the lattices satisfy certain symmetry properties necessary for isotropic behaviour.[8] The values of t_i are given in Table I for each lattice.

The macroscopic behaviour of the lattice Boltzmann method can be found by a procedure known as Chapman-Enskog analysis, where a multiple-scale analysis of the Taylor expansion of equation 3 is performed.[8,9] This analysis is performed under the assumptions of low excursions from equilibrium (all terms of order Ma^3 or higher are neglected), and the fluid being an isothermal perfect gas. It results in the equation of continuity and the compressible Navier-Stokes equation, with kinematic shear and bulk viscosities ν and ν' given directly by the relaxation time τ as

$$\nu = c_s^2\left(\tau - \frac{1}{2}\right), \tag{6a}$$

$$\nu' = \frac{2}{3}\nu. \tag{6b}$$

Because of the assumptions taken, these results are only valid in the isothermal limit of low Mach number.

Since the method results in a macroscopic behaviour consistent with the compressible Navier-Stokes equation under these constraints it should be possible to use for simulations of acoustics, since acoustic particle velocities tend to be very small compared to the speed of sound, and since the isothermal perfect gas approximation holds for small acoustic compressions and rarefactions.

In fluid mechanics, the lattice Boltzmann method has largely been used to simulate incompressible flow. It has therefore been associated with incompressible flow simulations, and there has unfortunately been relatively little research into wave propagation with the method.

III. POINT SOURCE

The author's method of researching acoustic wave propagation with the lattice Boltzmann method has been to perform benchmark comparisons with acoustic theory, where acoustic behaviour with known theoretical solutions is simulated with the lattice Boltzmann method.

Since wave propagation usually involves some sort of wave source, it is necessary to use a point source to perform these kinds of simulation. Unfortunately, no articles describing point sources for the lattice Boltzmann method with the BGK collision operator could be found. Only related concepts have been developed so far.[3,10]

The initial attempt by the author at creating a point source for the lattice Boltzmann method works by defining one or more nodes as source nodes, where the particle density ρ is forced to oscillate around an equilibrium density ρ_0,

$$\rho = \rho_0 + \rho_{\mathrm{src}} \sin\left(\frac{2\pi}{T}t\right). \tag{7}$$

In the simplest kind of free-field simulation, a point source is placed in the middle of a periodic 1D, 2D, or 3D system at equilibrium and is left to propagate waves outwards until the first wavefront approaches the boundary. The waves are then measured as a function of distance from the point source. The 2D system is sketched in Figure 2, and results in one to three dimensions are shown in Figure 3.

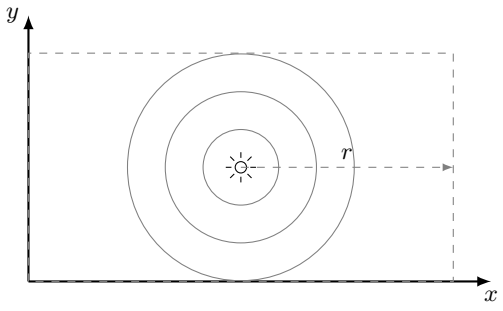

FIG. 2. Sketch for the two-dimensional case of the periodic system used in free-field simulations.

In Figure 3, the numerical results have been matched with modified (i.e. scaled and phase-shifted) steady-state analytical solutions of the system.[11] As can be seen, there is a very good visual match between the wave shape in

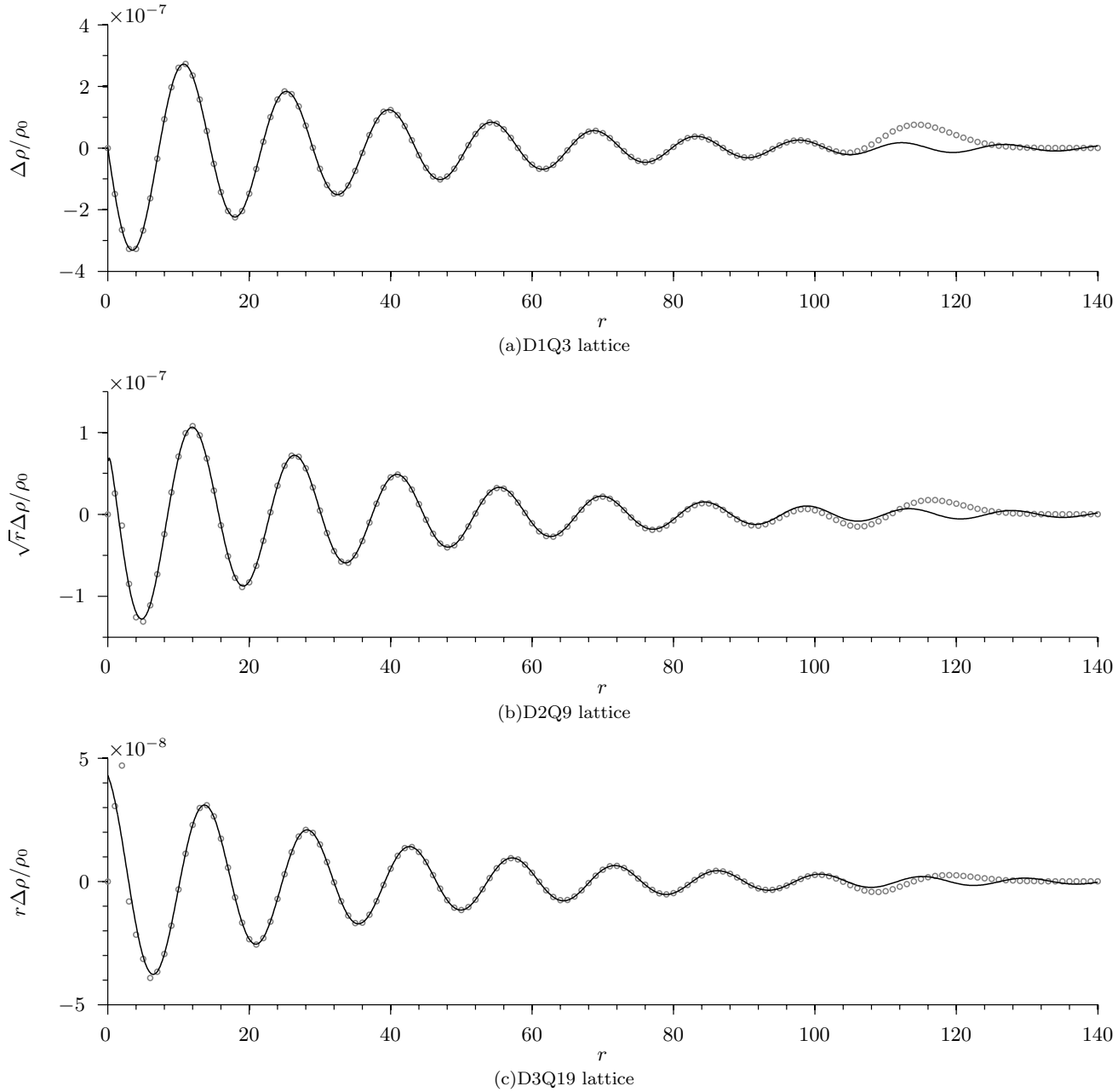

FIG. 3. *Non-steady-state lattice Boltzmann solution* of the radial field from a free-field point source in a viscous medium at $t = 200$ (circles), along with *steady-state analytical solution* of the same (lines), in one-, two- and three-dimensional lattices with $\tau = 0.75$. The point source used has a period $T = 25$ and an amplitude $\rho_{\mathrm{src}}/\rho_0 = 10^{-6}$. Note that in the two- and three-dimensional lattices, the solutions are scaled with $\sqrt{r}$ and r respectively, for visibility.

theory and simulation, and the rate of viscous damping seems correct.

Some problems with the point source were also found from these simulations. First, the radiated waves from the source do not have the expected amplitude compared with the source's amplitude. Also, in two and three dimensions (Figures 3(b) and 3(c)), there is some unexpected chaotic behaviour near the source — the neighbouring points are out of phase with the source, resulting in a propagated wave which has been phase-shifted compared to the source. These factors are the reasons for the aforementioned scaling and phase shift when matching analytical and simulated results.

The peaks which are visible around the first wavefronts around $r = 116$ in Figure 3 are not errors. When sound is radiated into a viscous fluid, a slowly decaying transient occurs around the first wavefront. This was described analytically in 1D by Blackstock in 1967,[12] and the simulated wavefront is compared with his analytical solution in Figure 4. As we can see, the agreement is very good. This illustrates the power of the lattice Boltzmann method to naturally simulate acoustic behaviour beyond

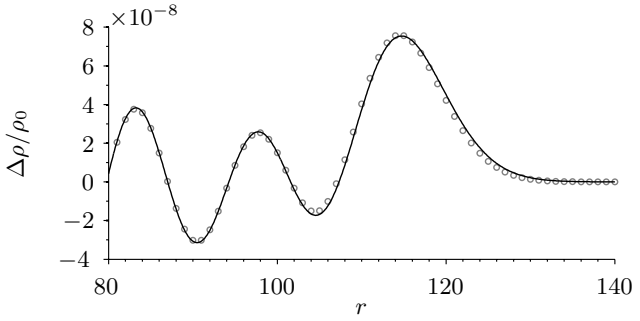

FIG. 4. First wavefront from Fig. 3(a) (circles), with analytical solution (Blackstock (1967)) of such a wavefront for a viscous medium (line).

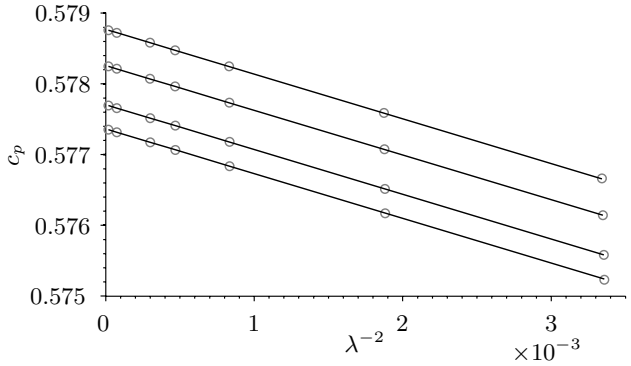

FIG. 5. Measured values of c_p (gray circles), with predictions based on a polynomial regression (black lines) for four different characteristic numbers. In ascending order, these lines represent $K = 1 \times 10^{-3}$, 5×10^{-3}, 8×10^{-3}, 1×10^{-2}.

the standard wave equation.

IV. DEVIATIONS IN PHASE VELOCITY AND ABSORPTION

The point source allows us to examine if spatially damped waves (i.e. waves which originate at a point and are affected by viscous absorption) in the lattice Boltzmann method behave as theoretically expected. By setting up a one-dimensional simulation such as the one described in the previous section we can measure the phase velocity and absorption coefficient of the outgoing waves.

An acoustic wave where the absorption is only affected by the viscous relaxation time

$$\tau_S = \frac{1}{c_s^2}\left(\frac{4}{3}\nu + \nu'\right) = 2\tau - 1 \tag{8}$$

can be shown to have a phase velocity of

$$c_p = c_s\left[1 + \frac{3}{8}(\omega\tau_S)^2\right] \tag{9}$$

and an absorption coefficient of

$$\alpha = \frac{\omega}{2c_s}(\omega\tau_S) \tag{10}$$

in the limit of $\omega\tau_S \ll 1$.[11]

If we define a characteristic number

$$K = \frac{\omega\tau_S}{2\pi} \tag{11}$$

we see that the phase velocity c_p should be constant if K is held constant. We also see that the quantity $\alpha T/K$ always should be constant.

Figure 5 shows the measured phase velocity as a function of λ^{-2} in four cases where K was held constant while T was varied, while Figure 6 shows $\alpha T/K$ as a function of λ^{-2} in the same cases. With both the phase velocity and absorption, there is a deviation from theory of order $\mathcal{O}(k^2 + K^2)$, so that the simulations agree with theory in the limit $k \to 0, K \to 0$.

The results of a regression analysis in λ^{-2} and K^2 on the results can be used to predict the values of c_p and

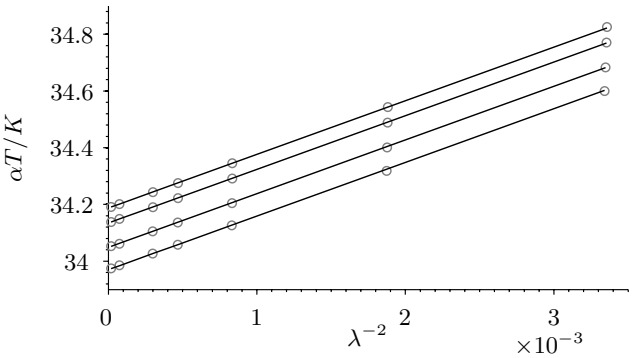

FIG. 6. Measured values of $\alpha T/K$ (gray circles), with predictions based on a polynomial regression (black lines). In descending order, these lines represent $K = 1 \times 10^{-3}$, 5×10^{-3}, 8×10^{-3}, 1×10^{-2}.

α *a priori* with an accuracy of respectively 0.001 55 % and 0.0176 % compared to the measurements performed here. The lines in Figures 5 and 6 are predictions based on these regressions.

V. UNIT CONSIDERATIONS

We have hitherto used lattice units, where the space and time steps have been normalised to 1. The lattice units can be related to a physical system through the physical time step Δt and physical space step Δx. The speed of sound and viscosity are related in lattice and physical units through

$$c_{s,\mathrm{phy}} = c_{s,\mathrm{lat}}\frac{\Delta x}{\Delta t}, \tag{12a}$$

$$\nu_{\mathrm{phy}} = \nu_{\mathrm{lat}}\frac{\Delta x^2}{\Delta t}. \tag{12b}$$

Inserting for the known lattice speed of sound and viscosity and solving for Δt and Δx, we find

$$\Delta t = \frac{\nu_{\text{phy}}}{c_{s,\text{phy}}^2(\tau - 1/2)}, \tag{13a}$$

$$\Delta x = \frac{\nu_{\text{phy}}\sqrt{3}}{c_{s,\text{phy}}(\tau - 1/2)}. \tag{13b}$$

Inserting physical values for air at 20 °C, this becomes

$$\Delta t = \frac{1.30 \times 10^{-10}}{\tau - 1/2} \text{ s}, \tag{14a}$$

$$\Delta x = \frac{7.73 \times 10^{-8}}{\tau - 1/2} \text{ m}, \tag{14b}$$

which shows that the time and space steps are restricted to orders of respectively *n*s and µm, since $\tau - 1/2$ cannot be arbitrarily close to zero for accuracy and stability reasons[13].

This problem does not occur when using the lattice Boltzmann method to simulate incompressible flow, since in that case the speed of sound is not a physically relevant quantity. This affords considerably more freedom in choosing units.[14]

VI. CONCLUSION

The lattice Boltzmann method has several desirable properties, in particular an inherent simplicity. The algorithm is easy to implement and use, and complex geometries of no-slip hard walls can be implemented simply by letting wall nodes bounce incoming particles back to their point of origin. Since each time step update is local to each node, the computational domain can be divided into subdomains handled by different processors, and it is possible to achieve a near-linear speedup in number of processors.[15]

It has been shown here that waves simulated with the lattice Boltzmann method suffer from deviations from theory of order $\mathcal{O}(k^2 + (\omega\tau_S)^2)$ in phase velocity and absorption, at least with the BGK collision operator. It may be possible to solve this problem by changing to a more advanced collision operator or by using an extended lattice.

Unfortunately, acoustic use of the lattice Boltzmann method seems to be limited to very high frequencies and very small geometries, limiting the area of usage to ultrasound microacoustics in fluids. Hopefully this can be rectified, but the manner in which this might be done is not yet clear to the author.

[1] G. McNamara and G. Zanetti, "Use of the Boltzmann Equation to Simulate Lattice-Gas Automata", Physical Review Letters **61**, 2332–2335 (1988).

[2] D. Haydock and J. M. Yeomans, "Lattice Boltzmann simulations of acoustic streaming", J. Phys. A **34**, 5201–5213 (2001).

[3] D. Haydock and J. M. Yeomans, "Lattice Boltzmann simulations of attenuation-driven acoustic streaming", J. Phys. A **36**, 5683–5694 (2003).

[4] J. M. Buick, C. L. Buckley, C. A. Greated, and J. Gilbert, "Lattice Boltzmann BGK simulation of nonlinear sound waves: the development of a shock front", Journal of Physics A **33**, 3917–3928 (2000).

[5] J. A. Cosgrove, J. M. Buick, D. M. Campbell, and C. A. Greated, "Numerical simulation of particle motion in an ultrasound field using the lattice Boltzmann model", Ultrasonics **43**, 21–25 (2004).

[6] A. R. da Silva, G. P. Scavone, and M. van Walstijn, "Numerical simulations of fluid-structure interactions in single-reed mouthpieces", J. Acous. Soc. Am. **122**, 1798–1809 (2007).

[7] B. R. Kucinschi, A. A. Afjeh, and R. C. Scherer, "On the application of the lattice Boltzmann method to the investigation of glottal flow", J. Acous. Soc. Am. **124**, 523–534 (2008).

[8] J. Latt, "Hydrodynamic limit of lattice Boltzmann equations", Ph.D. thesis, University of Geneva (2007).

[9] E. M. Viggen, "The lattice Boltzmann method with applications in acoustics", Master's thesis, Norwegian University of Science and Technology (2009).

[10] B. Chopard, P. O. Luthi, and J.-F. Wagen, "Lattice Boltzmann method for wave propagation in urban microcells", IEE Proc.-Microw. Antennas Propag. **144**, 251–255 (1997).

[11] L. E. Kinsler, A. R. Frey, A. B. Coppens, and J. V. Sanders, *Fundamentals of acoustics*, 4th edition (John Wiley & Sons) (2000).

[12] D. T. Blackstock, "Transient solution for sound radiated into a viscous fluid", J. Acous. Soc. Am. **41**, 1312–1319 (1967).

[13] B. Chopard, P. O. Luthi, and A. Masselot, "Cellular Automata and Lattice Boltzmann Techniques: An Approach to Model and Simulate Complex Systems", Advances in Complex Systems **5**, 103–246 (2002).

[14] J. Latt, "Choice of units in lattice Boltzmann simulations", Freely available online at `http://lbmethod.org/_media/howtos:lbunits.pdf`.

[15] "Palabos benchmarks", URL `http://www.lbmethod.org/palabos/benchmarks.html`.